Supporting Information

Directional Photonic Wire Mediated by Homo-Förster Resonance Energy Transfer on a DNA Origami Platform

Francesca Nicoli[1]*, Anders Barth[2]*, Wooli Bae[1], Fabian Neukirchinger[1], Alvaro H. Crevenna[2,3], Don C. Lamb[2‡] and Tim Liedl[1‡,]

[1] Department of Physics and Center for Nanoscience and [2] Department of Chemistry and Biochemistry and Center for Nanoscience, Ludwig-Maximilians-Universität, 80539 Munich;

[3] Current address: Instituto de Tecnologia Química e Biológica António Xavier, Universidade Nova de Lisboa, 2780-157 Oeiras, Portugal;

‡ Correspondence: tim.liedl@physik.lmu.de; d.lamb@lmu.de

* These authors contributed equally to this work

SI 1 – Nomenclature and schemes of all dyes arrangements described

Green to Red FRET Constructs	Name	Blue to Red FRET Constructs	Name
★☆☆★	G_1XXR	★★☆☆★	BG_1XXR
☆★☆★	XG_2XR	★☆★☆★	BXG_2XR
☆☆★★	XXG_3R	★☆☆★★	$BXXG_3R$
☆★★★	XG_2G_3R	★☆★★★	BXG_2G_3R
★☆★★	G_1XG_3R	★★☆★★	BG_1XG_3R
★★☆★	G_1G_2XR	★★★☆★	BG_1G_2XR
★★★★	$G_1G_2G_3R$	★★★★★	$BG_1G_2G_3R$

Table SI 1: *Nomenclature of all the linear dyes arrangements measured.*

SI 2 – Spectral properties of FRET pairs and dye-dye distance estimation

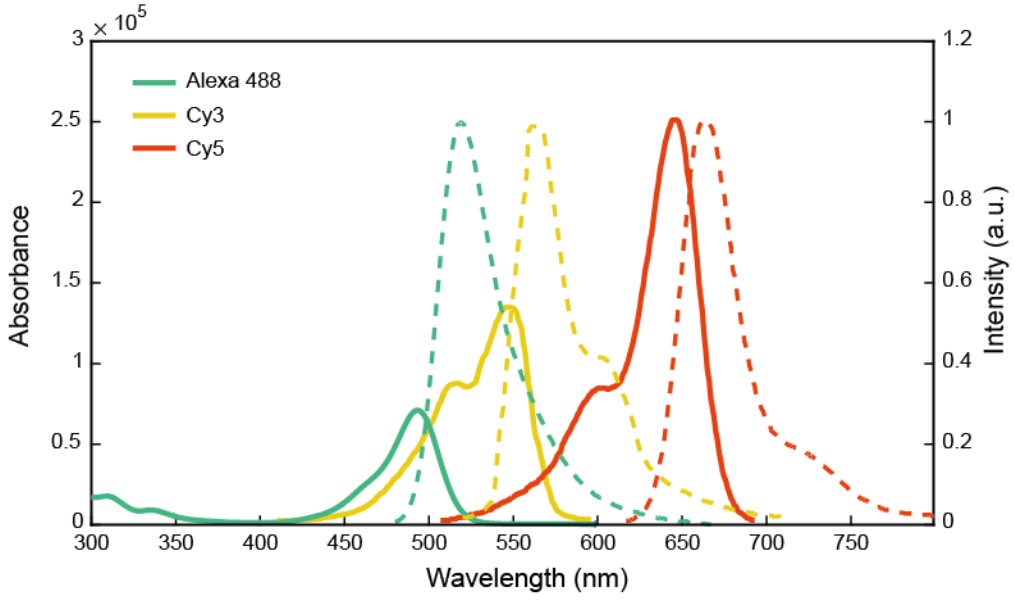

Figure S1: *Absorption (full line) and emission (dashed line) of dyes constructing the photonic wire*

The quantum yield (QY) values reported in Table S2 are taken from the referenced literature, while the overlap integral $J(\lambda)$ is calculated according to the measured absorption and emission spectra in Figure S1. The corresponding Förster radius is then calculated with the following formula[1]

$$R_0^6 = \frac{9000\ (\ln 10)\kappa^2 QY_D}{128\,\pi^5\,N\,n^4} * J(\lambda)$$

FRET pair	Overlap Integral J (nm^4/(M cm)	R_0 (nm)	Donor QY
Alexa488-Cy3	6.60x10^{15}	6.9	0.9[2]
Cy3-Cy3	3.71 x10^{15}	4.7	0.15[3,4]
Cy3-Cy5	7.86 x10^{15}	5.3	0.15[3,4]

Table S2: *Spectral properties of the FRET pairs. The overlap integral and R_0 are calculated from spectra in figure S1, for quantum yield values refer to the cited literature.*

To estimate the dye-dye distance on the DNA origami structure, we assume as inter-helical distance the value of 2.7 nm, the value was taken from Fischer *et al*[5] where the same DNA structure used in our work was measured by means of SAXS (small angle x-ray scattering). The error arising from those measurements is of the order of 0.02 Å, so we assume the main source of error to be the dyes fluctuations on the DNA origami. All the fluorophores are linked to the DNA via NHS Ester coupling with a 6-Carbon chain of estimated length of about ~0.4 nm.[6] Therefore, we calculate the dye-dye distance error to be $\sigma_d = \sqrt{2 * 0.4^2}\ nm = 0.57\ nm$

SI 3 – Direct excitation of Cy5 – control

To determine the amount of Cy5 direct excitation by the incident beam centered at 520 nm in bulk measurements, we perform a control experiment consisting in a mixture of Cy3 and Cy5 labeled DNA staples. The staples are mixed in a 3:1 Cy3:Cy5 ratio, corresponding to the $G_1G_2G_3R$ construct. The distance between Cy3 and Cy5 in solution is large and does not allow energy transfer between the green and red dyes. Hence, the emission spectrum gives an estimation of the direct excitation of Cy5 after Cy3

excitation when no FRET occurs (see main manuscript Figure 2). Furthermore, we estimate the absorption of Cy5 at 520 nm to be less than $0.02 * \varepsilon_{cy5}$, where ε_{cy5} is the extinction coefficient of the dye.

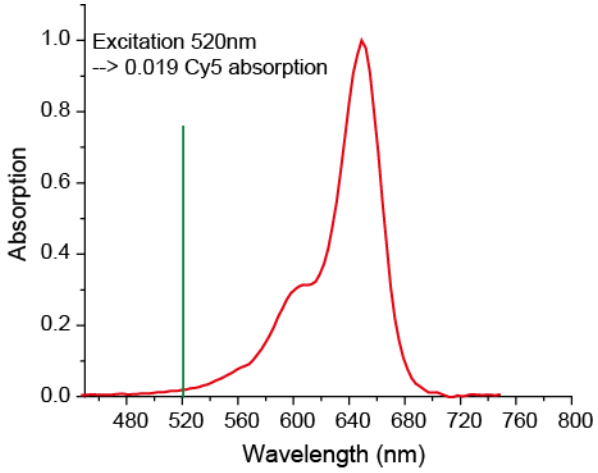

Figure S2: *Normalized Cy5 absorption spectrum and excitation wavelength at 520 nm.*

SI 4 – Cy3/Cy5 energy transfer efficiency estimation from bulk measurements

Bulk steady-state fluorescence spectroscopy measurements give us information about the average emission of the sample under consideration. In our case it is impossible to calculate the exact energy transfer efficiency, because we cannot account for the fluorescence coming from structures that contain a different number of dyes than the target construct. To estimate the energy transfer, we simply consider the ratio-metric FRET efficiency, defined as the donor emission (I_{Cy3}), divided by the total emission of donor and acceptor (I_{Cy5}) at their maximum.

$$E_{Bulk} = \frac{I_{Cy3}}{I_{Cy3} + I_{Cy5}}$$

For constructs with Cy3 and Cy5 dyes only, since we excite Cy3 at 520 nm we assume the direct excitation of Cy5 to be negligible (Figure S2) and correct the Cy5 emission only for the spectral overlap with Cy3. We consider the resulting spectrum as the linear sum of Cy3 and Cy5 emission; we correct for the spectral overlap by subtracting 3% of the Cy3 emission signal at its maximum from the acceptor channel measured at 667 nm $I_{Cy5} = I^*_{Cy5} - 0.03 * I_{Cy3}$, where I^*_{Cy5} represents the uncorrected acceptor emission counts.

SI 5 – Efficiency enhancement calculations

In our calculations, we assume that, if homo-FRET dyes were transferring energy to the acceptor independently, the green to red energy transfer of the constructs carrying multiple Cy3 dyes, E_{Tot}, should be equal to the average of the hetero-FRET efficiency of each Cy3/cy5 pair:

$$E_{Aver} = \frac{\sum_0^n E_i}{n} \lessgtr E_{Tot}$$

FRET efficiency enhancement, ΔE, is calculated as the difference between the efficiency of the multiple Cy3 labeled structure, E_{Tot}, and the average efficiency of the single constructs, E_{Aver}:

$$\Delta E = E_{Tot} - E_{Aver}$$

SI 6- Single-molecule fluorescence burst measurements and analysis

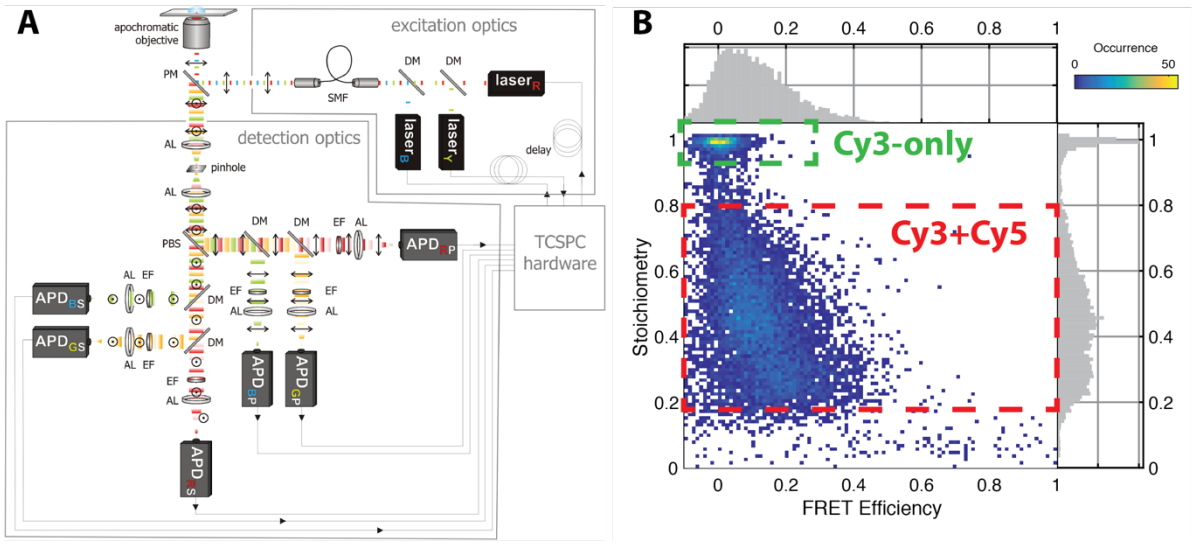

Figure S3: *Single-molecule experiments and data analysis. A) Schematic of the confocal microscope used for the single-molecule measurements. Three laser are alternated on the nanosecond timescale to excite molecules freely diffusing through the confocal volume. The collected fluorescence signal is passed through a pinhole and split by polarization and color. Single photons are detected on avalanche photodiodes (APD) and the signal is processed by time-correlated single photon counting (TCSPC) hardware. DM: dichroic mirror, SMF: single-mode fiber, PM: polychroic mirror, AL: achromatic lens, PBS: polarizing beam splitter, EF: emission filter. B) Example for the single-molecule sorting based on FRET efficiency and stoichiometry thresholds to distinguish double-labeled from Cy3-only molecules.*

Cy3-only labeled molecules are separated from Cy3-Cy5 labeled molecules using the stoichiometry parameter defined by:

$$S = \frac{F_{GG} + F_{GR}}{F_{GG} + F_{GR} + F_{RR}}$$

Here, *F* is the fluorescence intensity in the donor channel (GG), FRET channel (GR) and acceptor channel (RR). Cy3-only labeled molecules are selected based on a stoichiometry threshold S >= 0.95, while dual-color labeled molecules are selected by 0.2<=S<=0.8. Additionally, artifacts due to photobleaching are excluded by application of the ALEX-2CDE filter.[7]

For the calculation of the FRET efficiency, photon counts are corrected for uniform background signal. The signal in the FRET channel is additionally corrected for crosstalk from the donor fluorophore ($ct = 0.13$) and direct excitation of the acceptor fluorophore by the donor excitation laser ($de = 0.19$).[8]

$$E = \frac{F_{GR} - ct * F_{GG} - de * F_{GR}}{F_{GG} + F_{GR} - ct * F_{GG} - de * F_{GR}}$$

The reported FRET efficiencies are not corrected for the differences in the detection efficiency and quantum yield of donor and acceptor fluorophore, since such correction is only possible if the quantum yield of the dyes is either invariant or known a priori. Since clearly the donor showed changing quantum yield depending on labeling position and the presence of homo-FRET acceptors, this correction could not be applied here.

	G_1XXR	**XG_2XR**	**XXG_3R**	**G_1G_2XR**	**G_1XG_3R**	**XG_2G_3 R**	**$G_1G_2G_3$ R**
E	0.06	0.13	0.45	0.09	0.33	0.40	0.28
Cy3 only [%]	10.5	7.8	7.2	10.7	21.8	7.7	22.7

Table S3: *Results from single molecule FRET measurements. Given are the FRET efficiency of dual-color labeled molecules as estimated from the intensity information, as well as the percentage of molecules that had no active acceptor (Cy3 only).*

Molecule-wise fluorescence lifetimes are determined by fitting each single-molecule event with a mono-exponential model function. The molecule-wise anisotropy r is calculated from background-corrected photon counts for donor- and acceptor signal by:

$$r = \frac{G * F_{\parallel} - F_{\perp}}{G * F_{\parallel} + 2F_{\perp}}$$

Here, G is a correction factor accounting for slightly different detection efficiencies of the parallel and perpendicular channel ($G = 1.05$ for the green detection channel, $G = 1.15$ for the red detection channel).

SI 7- Bulk efficiency corrected by donor only species from single-molecule measurements

	E bulk	*% donor only*	*Corrected E bulk*
G_1XXR	0.05	10.50	0.06
XG_2XR	0.12	7.80	0.13
XXG_3R	0.33	7.20	0.36
XG_2G_3R	0.29	10.70	0.32
G_1G_2XR	0.07	21.80	0.09
G_1XG_3R	0.21	7.70	0.23
$G_1G_2G_3R$	0.19	22.70	0.25

Table S4: *Bulk fluorescence efficiencies determined using the amount of donor-only species measured from SM experiments.*

SI 8- Fluorescence anisotropy analysis

The sub-ensemble time-resolved anisotropy decays are calculated from the cumulative intensity decays by:

$$r(t) = \frac{G * I_{\parallel}(t) - I_{\perp}(t)}{G * I_{\parallel}(t) + 2I_{\perp}(t)}$$

Generally, the fluorescence anisotropy decays exponentially on the sub-nanosecond timescale due to the rotation of the fluorophore attached the macromolecules.

$$r(t) = (r_0 - r_\infty)\exp\left(-{}^{t}/_{\rho}\right) + r_\infty$$

The initial anisotropy r_0 is dependent on intrinsic properties of the fluorophore and takes a maximum value of 0.4. The rotational correlation time ρ reports on the rotational freedom of the fluorophore and the residual anisotropy r_∞ reports on the rotation of the macromolecule itself.

The observed “dip-and-rise” behavior is described by a superposition of a two distinct anisotropy decays with different associated fluorescence lifetimes, leading to time-dependent changes of the relative

contributions to the anisotropy decay (see main text and Stennett *et al*. [9]). The full model function is then given by:

$$r(t) = A_1(t)\left[\left(r_0 - r_{\infty,1}\right)\exp\left(-{}^{t}/_{\rho_1}\right) + r_{\infty,1}\right] + \left(1 - A_1(t)\right)\left[\left(r_0 - r_{\infty,2}\right)\exp\left(-{}^{t}/_{\rho_2}\right) + r_{\infty,2}\right]$$

Here, the intensity-fraction of the first species, $A_1(t)$, is given by:

$$A_1(t) = \frac{I_{0,1}e^{-t/\tau_1}}{I_{0,1}e^{-t/\tau_1} + I_{0,2}e^{-t/\tau_2}}$$

For simplicity, we only assume two independent species, although the lifetime analysis considers three components. The lifetimes of the two species are determined from the intensity decay by fitting with a biexponential model function and fixed for the analysis of the anisotropy decay. 95% confidence intervals for the residual anisotropy are determined based on the Jacobian matrix using the nlparci function in MATLAB.

Anisotropy decays of all Cy3 only labeled constructs are depicted in figure S4. Data points are fitted (solid lines) according to the model described above. In all construct carrying multiple Cy3 dyes a decrease in anisotropy is observed, indicating the occurrence of homo-FRET.

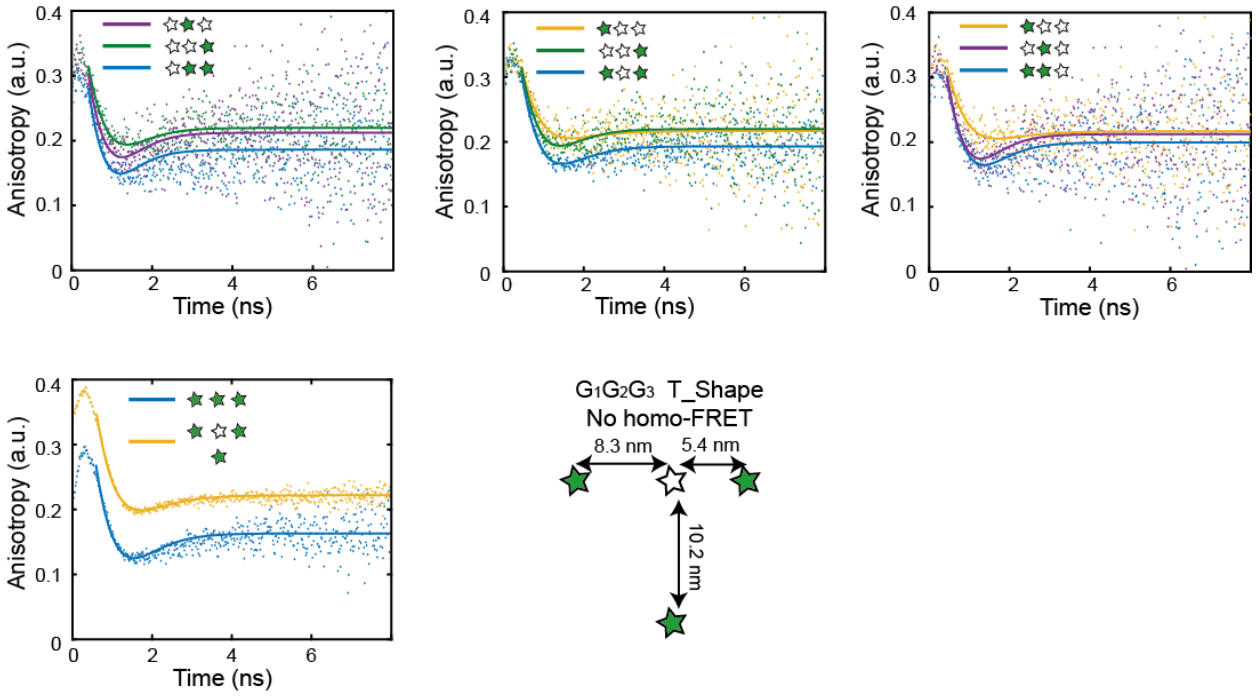

Figure S4: *Anisotropy decays of Cy3 only labeled structures. Construct $G_1G_2G_3$ is compared with a control construct, where all three green dyes are present, but at distances that does not allow any homo-FRET.*

SI 9- Fluorescence lifetime analysis

Fluorescence decays are extracted from single-molecule measurements by combining photons from all selected molecules (sub-ensemble analysis). Parallel and perpendicular intensity decays are combined to eliminate the contribution of rotation by:

$$I(t) = G * I_{\parallel}(t) + 2I_{\perp}(t)$$

The cumulative decay histograms are fitted using a model with three lifetime components.

$$I(t) = I_0 \sum_{i=1}^{3} F_i exp(-t/\tau_i), \text{where } \sum F_i = 1$$

To account for the instrument response function of the detectors, the analytical decay is convoluted with the measured instrument response function *(IRF)*, yielding the model function *M(t)*:

$$M(t) = IRF(t) \otimes I(t)$$

The intensity-averaged fluorescence lifetime is calculated from the fitted parameters as:

$$\langle \tau \rangle = \frac{\sum F_i \tau_i^2}{\sum F_i \tau_i}$$

Confidence intervals for the fitted intensity-averaged lifetime are determined using bootstrapping by performing independent analysis of 10 random samples of subsets of bursts containing 25% of the total population.

The lifetime data for Cy3 only labeled constructs and FRET constructs, Cy3 and Cy5 labeled, are presented in figure S6 and S7 respectively. The data are depicted as scattered points and the fitting function as a line. Lifetime values calculated from the fitting functions are summarized in table S5 for Cy3 only constructs and in Table S6 for FRET constructs. Constructs carrying Cy3 only show a decrease in lifetime when multiple green dyes are present. This effect is discussed in the main manuscript, related to the three-Cy3 construct. Dyes undergoing hetero-FRET present a further reduction in lifetime due to FRET.

The extracted lifetime values for the short ($0.33 \pm 0.08\ ns$) and long ($2.60 \pm 0.01\ ns$) lifetimes are in very good agreement with the lifetimes of free Cy3 (0.2-0.3 ns) and Cy3b (2.7-2.8 ns). The presence of distinct lifetimes and rotational states of Cy3 on the origami constructs is additionally supported by the observed anisotropy decays (as described in the main) and the burst-wise lifetime distributions that show a broad distribution of the molecule-wise lifetimes (shown in Figure S5). Thus, we assign the fast and slow lifetime components to rotationally free and rotationally hindered (due to the interaction with the origami surface) Cy3 molecules, respectively. We accordingly attribute the third intermediate component to molecules that experience partial inhibition of rotation.

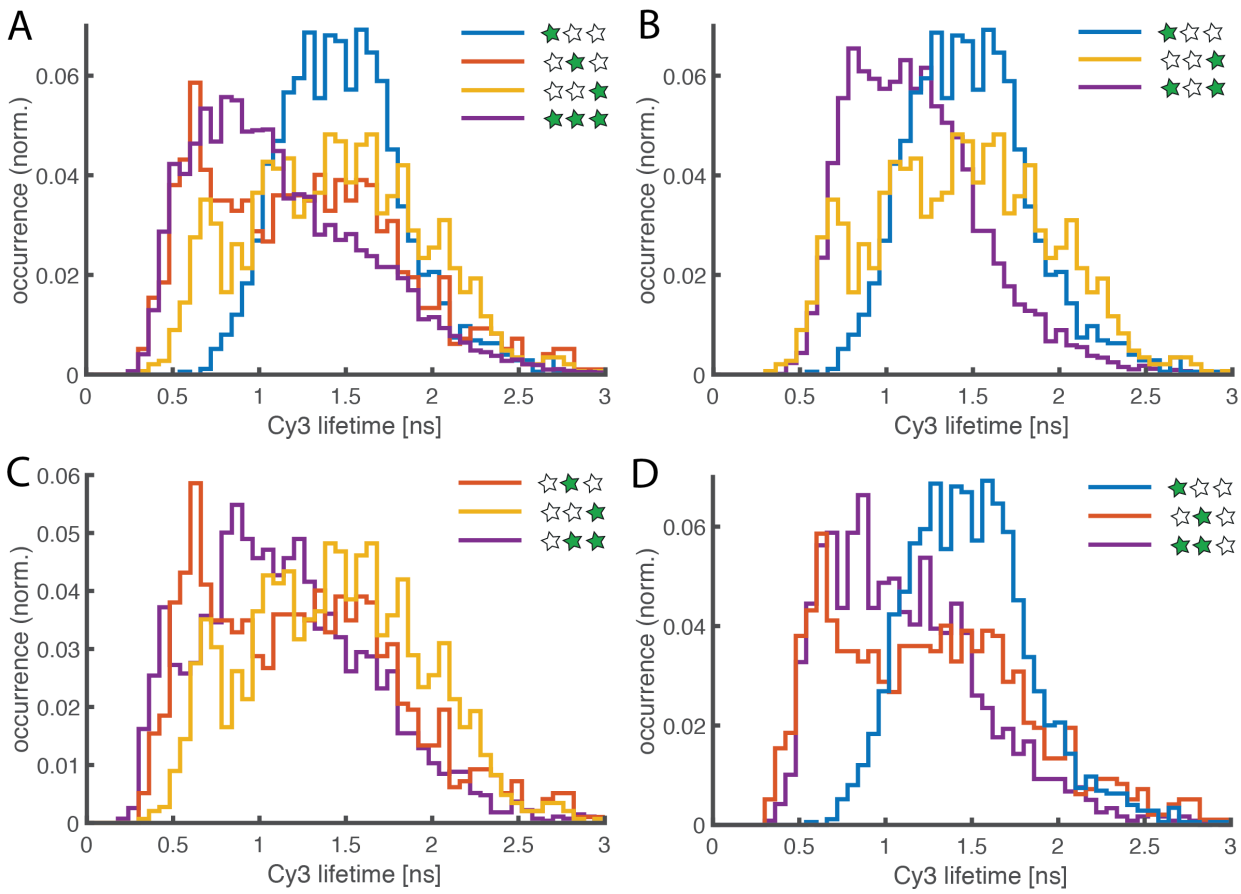

Figure S5: *Molecule-wise distributions of the fluorescence lifetime of Cy3 in the absence of the acceptor for the given constructs. Each panel compares the distributions for multi-Cy3 constructs with the respective single-Cy3 constructs.*

We have tested the use of a stretched exponential and found that the fit quality as measured by the reduced χ^2_{red} criterion is worse as compared to the three-exponential fit. To compare the two model functions, we computed the Bayesian information criterion (BIC) for both models and found that the three-exponential model function consistently yields the lower value for the BIC over all data sets, and is thus to be preferred.

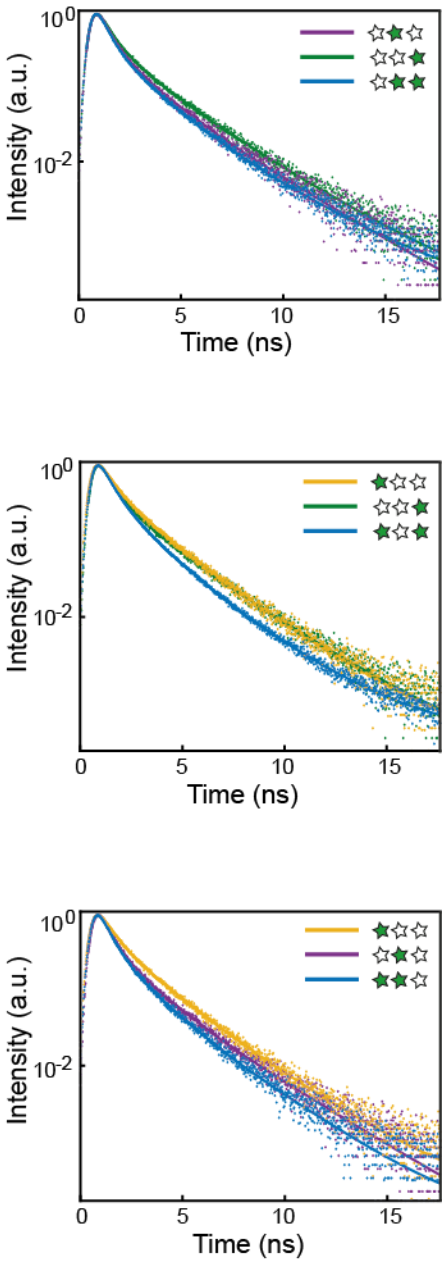

Figure SI 6: *Lifetime measurements and fits of constructs carrying only Cy3 dyes. Construct $G_3G_2G_1$ is presented in the main manuscript.*

	G_1XX	XG_2X	XXG_3	G_1G_2X	G_1XG_3	XG_2G_3	$G_1G_2G_3$
τ_1	0.39	0.29	0.32	0.30	0.35	0.32	0.31
τ_2	1.29	1.01	1.12	1.02	1.17	1.20	1.04
τ_3	2.59	2.59	2.61	2.49	2.68	2.84	2.66
F_1	0.53	0.65	0.62	0.64	0.61	0.71	0.68
F_2	0.33	0.26	0.26	0.29	0.33	0.24	0.28
F_3	0.14	0.09	0.12	0.07	0.06	0.05	0.04
$\langle\tau\rangle$	1.57	1.34	1.52	1.20	1.27	1.27	1.09

Table S5: *Lifetime analysis of Cy3-only labeled constructs using a three-exponential model function. Lifetimes are given in ns. $\langle\tau\rangle$ is the intensity-averaged lifetime.*

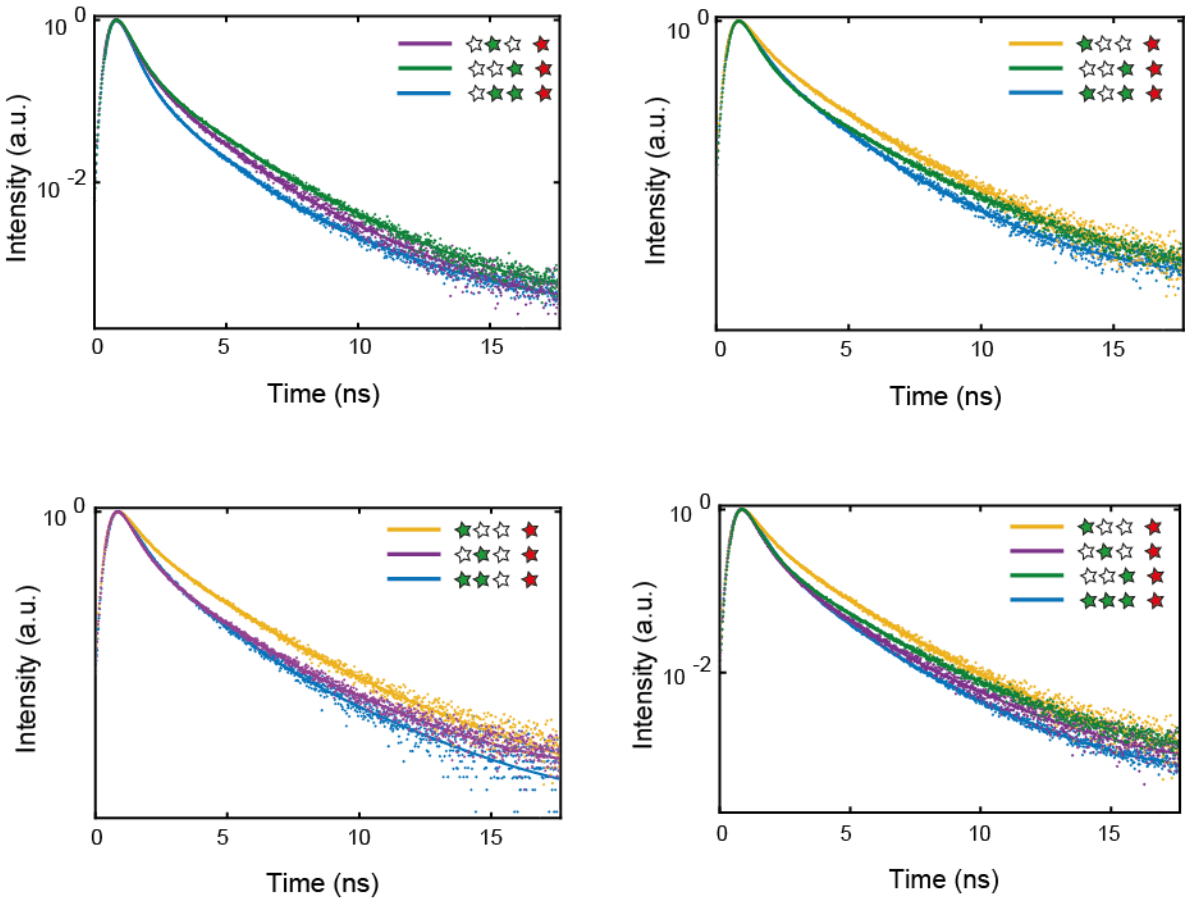

Figure S7: *Fluorescence decays of all Cy3/Cy5 FRET constructs.*

	G_1XXR	XG_2XR	XXG_3R	G_1G_2XR	G_1XG_3R	XG_2G_3R	$G_1G_2G_3R$
τ_1	0.38	0.30	0.31	0.32	0.33	0.29	0.36
τ_2	1.29	1.05	1.00	1.04	1.12	1.03	0.97
τ_3	2.77	2.76	2.61	2.73	2.87	3.14	2.56
F_1	0.62	0.75	0.75	0.72	0.70	0.83	0.68
F_2	0.32	0.22	0.20	0.26	0.27	0.15	0.29
F_3	0.06	0.03	0.05	0.02	0.03	0.01	0.03
$\langle\tau\rangle$	1.35	1.01	1.10	0.95	1.03	0.84	0.95

Table S6: *Lifetime analysis of Cy3-Cy5 labeled constructs using a three-exponential model function. Lifetimes are given in ns. $\langle\tau\rangle$ is the intensity-averaged lifetime.*

SI 10 – Direct transfer from Alexa488 to Cy5

We perform a control measurement to exclude the possibility of direct transfer between the blue donor to the red acceptor. When we excite the construct BXXXR at 490 nm we observe no emission from the 660-670 nm region of the spectrum, indicating that no energy is directly transferred or not partial excitation of Cy5 is taking place. Subsequently we excite the same sample at 640 nm and we detect Cy5 emission to confirm the presence of the acceptor dye.

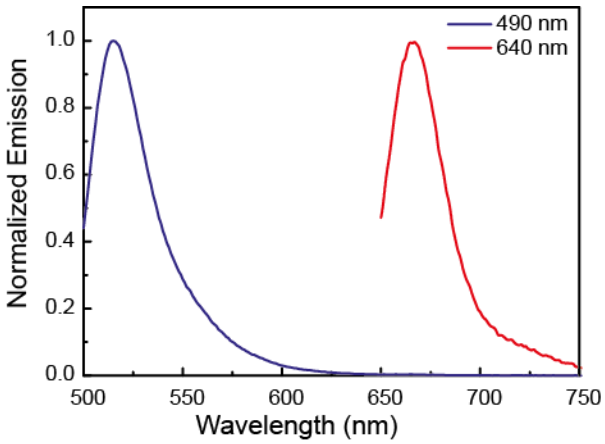

Figure S8*: Emission spectra of the construct BR, containing only Alexa488 and Cy5. The sample was excited at two different wavelengths, 490 nm (blue line) and 640 nm (red line). The blue spectrum shows emission from Alexa488 only, indicating that no transfer Cy5 is occurring, even though the presence of the acceptor is confirmed by the red spectrum.*

SI 11 - Three-color single-molecule data analysis

For the three-color single-molecule experiments we employ alternating excitation of the three dyes on the nanosecond timescale. Molecules with active donor, transmitter and acceptor dye are selected based on the labeling stoichiometries S_{GR}, S_{BG} and S_{BR}, where the quantities S_{BG} and S_{BR} are defined based on the background-corrected fluorescence signal after blue excitation, denoted by F_{BB}, F_{BG} and F_{BR} for the signal in the blue, green and red channel after excitation of the blue fluorophore.

$$S_{BG} = \frac{F_{BB} + F_{BG} + F_{BR}}{F_{BB} + F_{BG} + F_{BR} + F_{GG} + F_{GR}} \qquad S_{BR} = \frac{F_{BB} + F_{BG} + F_{BR}}{F_{BB} + F_{BG} + F_{BR} + F_{RR}}$$

The overall apparent energy transfer efficiency from the blue dye to the red acceptor dye is measured by the fraction of red photons after blue excitation, given by:

$$E_{B\to R} = \frac{F_{BR}}{F_{BB} + F_{BG} + F_{BR}}$$

In analogy to the bulk measurements, we choose the above defined apparent transfer efficiency $E_{B\to R}$ to report on the transfer process. Note that this quantity is biased by artefacts of crosstalk and cross-excitation. Most importantly, this quantity will scale with the number of Cy3 dyes due to the possibility of direct excitation of Cy3 by the blue laser, leading to false positive signal in the channel F_{BR}. However, relative comparisons are still valid.

Additionally, we performed sub-ensemble fluorescence lifetime analysis of the blue donor dye Alexa488. We selected molecules which only possessed the blue dye using stoichiometry threshold $S_{BG} > 0.98$ and $S_{BG} > 0.98$ to determine the donor-only lifetime $\tau_{B,0}$, and determined the fluorescence lifetime in the presence of Cy3 and Cy5 $\tau_{B,GR}$ from the triple-labeled molecules. The total FRET efficiency away from the blue dye $E_{B\to G+R}$ is then given by:

$$E_{B\to G+R} = 1 - \frac{\tau_{B,GR}}{\tau_{B,0}}$$

The results are summarized in Table S7 and S8.

	$BG_3G_2G_1R$	BG_3XXR	BXG_2XR	$BXXG_1R$	BG_3XG_1R	BXG_2G_1R	BG_3G_2XR	$BXXXR$
ET BR [%]	9.8	5.1	2.8	3.7	9.5	4.8	5.6	1.1
+/-	3.7	2.0	1.9	2.2	3.2	2.7	2.2	0.6

Table S7: *Apparent efficiency of energy transfer (ET BR) in single-molecule measurements measured by the fraction of red photons after blue excitation. Given are the mean values and standard deviations of the distributions.*

	$BG_3G_2G_1R$	BG_3XXR	BXG_2XR	$BXXG_1R$	BG_3XG_1R	BXG_2G_1R	BG_3G_2XR
$\boldsymbol{\tau_{B,0}}$ $(\boldsymbol{ns})$	3.98	4.01	4.02	3.90	3.77	3.99	3.85
$\boldsymbol{\tau_{B,GR}}$ $(\boldsymbol{ns})$	2.01	1.93	3.49	3.74	2.05	3.35	1.72
$\boldsymbol{E}$	0.495	0.519	0.132	0.041	0.456	0.160	0.55

Table S8: *Single-molecule fluorescence lifetime analysis of Alexa488. Given are the Alexa488 lifetime in the absence of Cy3 and Cy5 ($\boldsymbol{\tau_{B,0}}$) and in the presence of Cy3 and Cy5 ($\boldsymbol{\tau_{B,GR}}$). The total efficiency of energy transfer away from Alexa488 ($\boldsymbol{E}$) is calculated from the lifetime by $\boldsymbol{E = 1 - \frac{\tau_{B,GR}}{\tau_{B,0}}}$. Lifetimes are given in nanoseconds.*

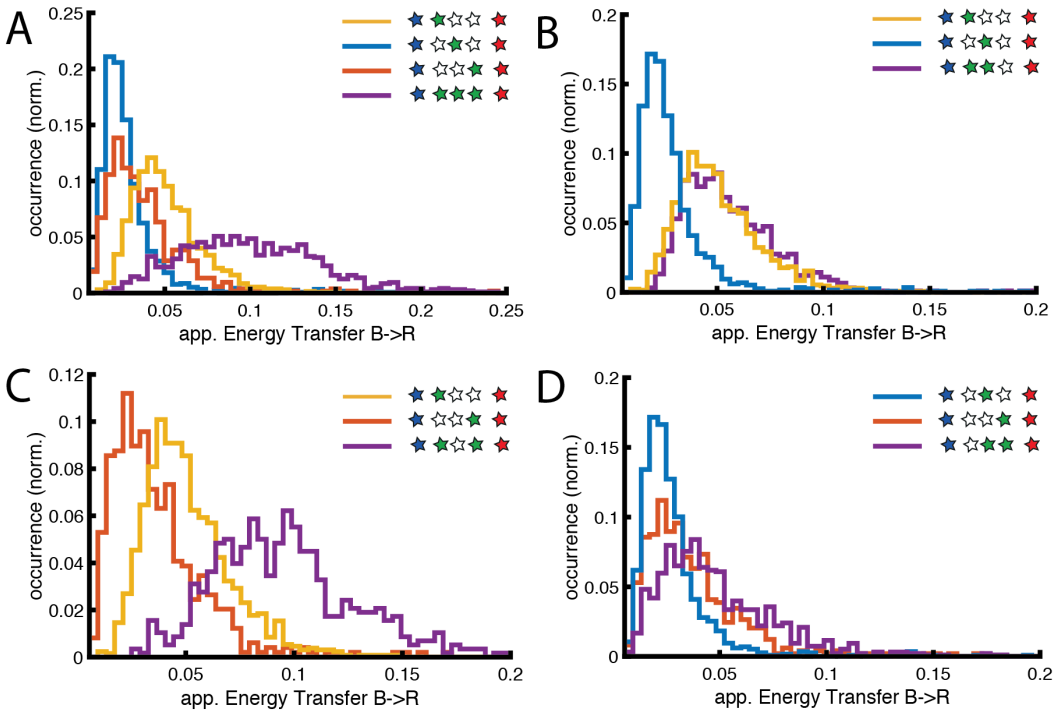

Figure S9: *Comparison of the apparent energy transfer efficiency from the blue donor dye to the red acceptor dye for differently labeled three-color constructs.*

SI 12 – Full PW energy transfer estimation from bulk measurements

In case of three-color FRET, the emission spectrum is complex, since it results from the convolution of the superposition of three different spectra, partially overlapping with each other. To estimate the emission from each single dye component, we perform a linear decomposition of the three spectra, Alexa488, Cy3 and Cy5. Varying the weight of each spectrum, we extract the relative emission of all the components (Figure S10).

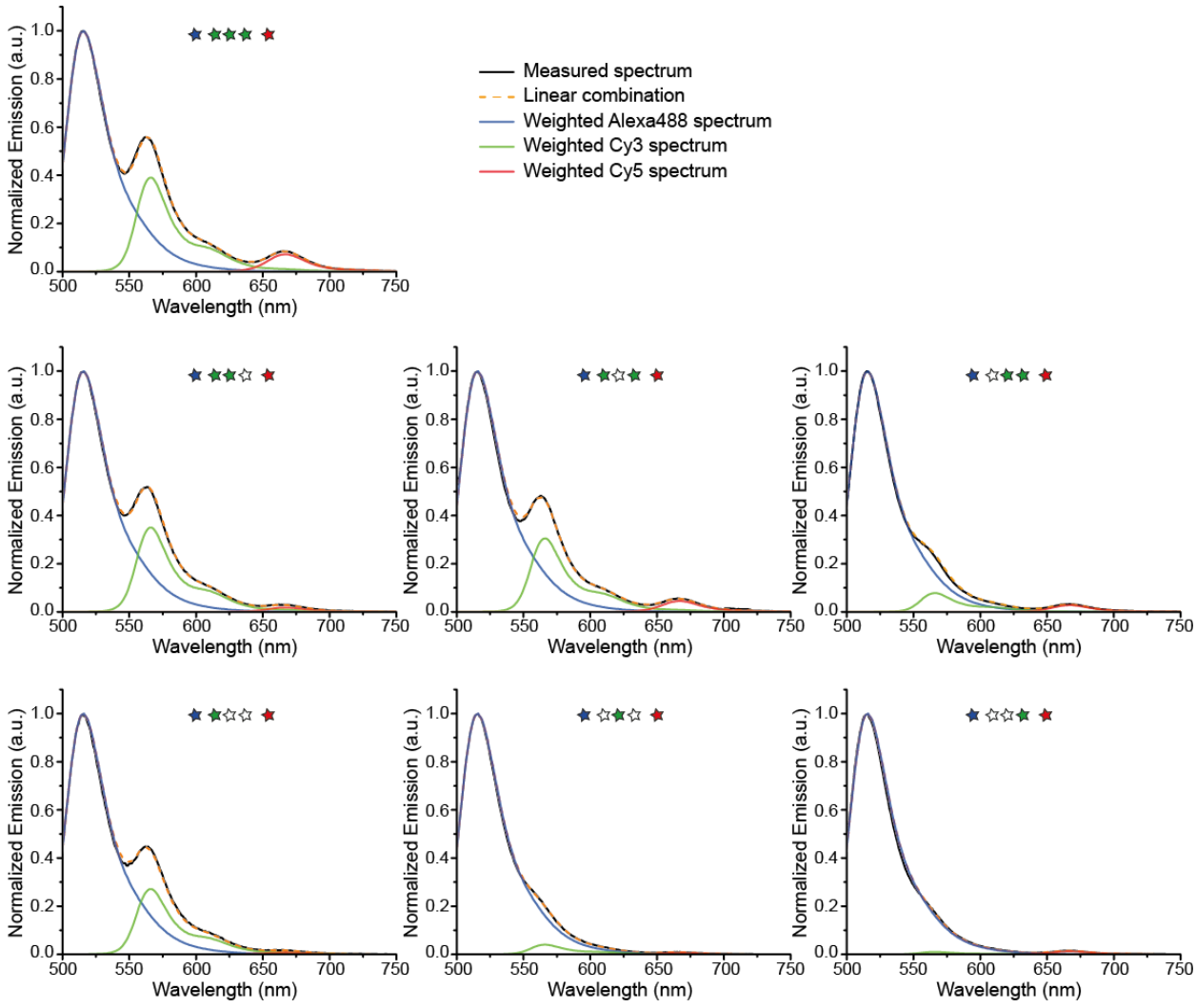

Figure S10: *tree-color FRET cascades. All the spectra are normalized by Alexa488 emission. The contribution of each dye to the total spectrum is evaluated through a linear combination of the emission of each cascade dye (dashed orange line). Each weighted spectrum is also represented, alexa488 (blue), Cy3 (green), Cy5 (red).*

Furthermore, in order to efficiently excite Alexa488, at 490 nm, we generate a non-negligible amount of direct excitation of Cy3. It is possible to shift the excitation wavelength further into the blue region of the spectrum, but only for constructs with an efficient blue to red transfer. In fact, in the energy cascades with only one intermediate dye, the blue to red transfer is very inefficient and the signal of Cy5 becomes comparable with the noise. Therefore, for excitation at 490 nm, we estimate the apparent

energy transfer efficiency of the constructs as the ratio between red intensity peak ($I_{Peak\ (Cy5)}$) and the sum of the intensity peak of blue ($I_{Peak\ (Alexa488)}$), green ($I_{Peak\ (Cy3)}$) and red fluorophore. The intensity values are corrected for cross-talk between dyes (see linear decomposition of spectra Figure S10), but not for the partial direct excitation of Cy3.

$$E = \frac{I_{Peak\ (Cy5)}}{I_{Peak\ (Alexa488)} + I_{Peak\ (Cy3)} + I_{Peak\ (Cy5)}}$$

We focus on the comparison between different numbers of intermediate dyes to prove that the energy in the PW is indeed transferred through the homo-FRET chain.

Constructs	E Bulk
BG_1XXR	0.006
BXG_2XR	0.006
$BXXG_3R$	0.013
BG_1G_2XR	0.013
BG_1XG_3R	0.025
BXG_2G_3R	0.033
BG_1G_2G3R	0.049

Table S9: Blue *to red transfer efficiencies from bulk emission spectroscopy*

To prove that the energy transfer Alexa 488 and Cy5 is indeed mediated by Cy3 dyes and not a result of direct excitation of Cy3, we performed a control measurement on the full PW where we shifted the excitation from 490 nm to 460 nm (Figure S11). In this case the signal and the signal-to-noise significantly decrease, but the emission from the red dye can still be detected.

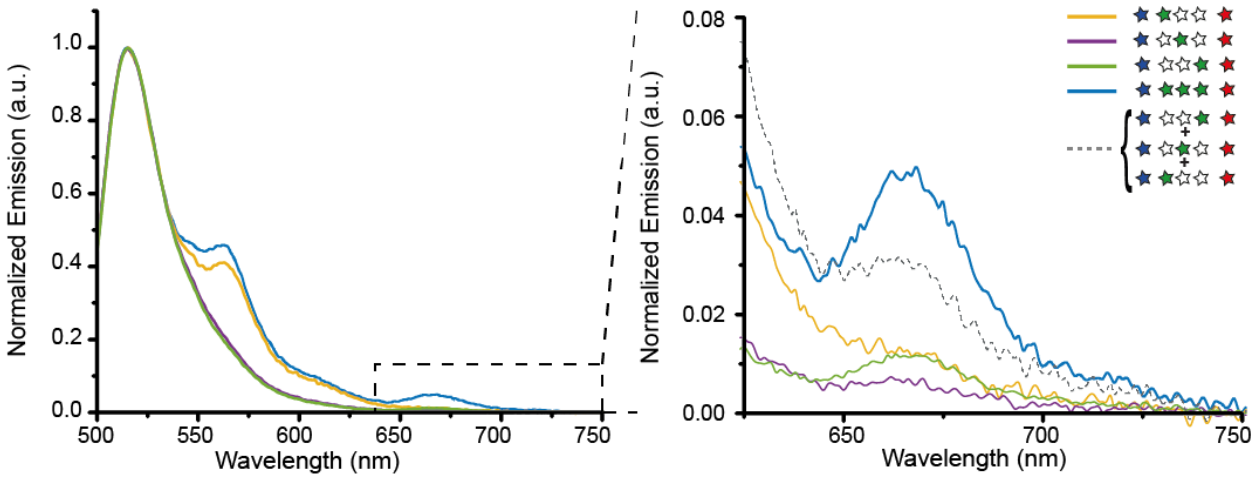

Figure S11: *Control measurement of the three-color cascade. (Left) Normalized emission spectra after Alexa488 excitation at 460 nm. (Right) Zoom in into the Cy5 emission. Constructs with only one green dye do not show a significant emission of the red acceptor. Cy5 emission appears when all three Cy3 dyes are present. The gray dashed line represents the arithmetic sum of the red signals from BG_1XXR, BXG_2XR and $BXXG_3R$, which is significantly lower than the red emission from $BG_1G_2G_3R$.*

SI 13 – Monte Carlo calculations

Using Monte Carlo simulations, we calculated emission for the three-color FRET cascade. In the calculations, we assumed 23% of direct excitation of Cy3 by the incident light. The transfer efficiency of each wire was calculated as the ratio between Cy5 emission and total emission i.e. sum of Alexa488, Cy3 and Cy5 emission.

	Calculated Emission			**Efficiency**
	Alexa488	Cy3	Cy5	B->R
$BG_1G_2G_3R$	0.5023	0.3069	0.0376	0.044
$BXXG_3R$	1.8155	0.0625	0.0186	0.010
BXG_2XR	1.5	0.1015	0.0069	0.004
BG_1XXR	0.6352	0.2443	0.0057	0.006

Table S10: *Emission values obtained from Monte Carlo calculations of the partial and full PW. Efficiencies were calculated as described above.*

SI 14 – Origami structure design

The origami structure consists of a 3-layer block on a square lattice based design. The position of the fluorophores in the structure is marked with a star and all the dyes are by design located on the surface of the origami block. The Cy3 molecule of strand G_2 could not be placed in a perfect line with the other dyes due to the antiparallel nature of DNA strands. In fact, on helix 15 (see Figure S12) the long viral scaffold is on the block surface at the ideal perfect linear alignment with the other dyes. The Cy3 molecule location is consequentially shifted by half helical turn, so that it is located on the origami surface.

The origami structure was folded by mixing 20 nM ssDNA scaffold (derived from phage M13 mp18 variant p8064) with a 10X excess sort staple strands (15 to 50 bases long) in 10 mM Tris, 1 mM EDTA and 16 mM $MgCl_2$ buffer. The mixture was annealed with a 16 hour temperature ramp from 65°C to room temperature.

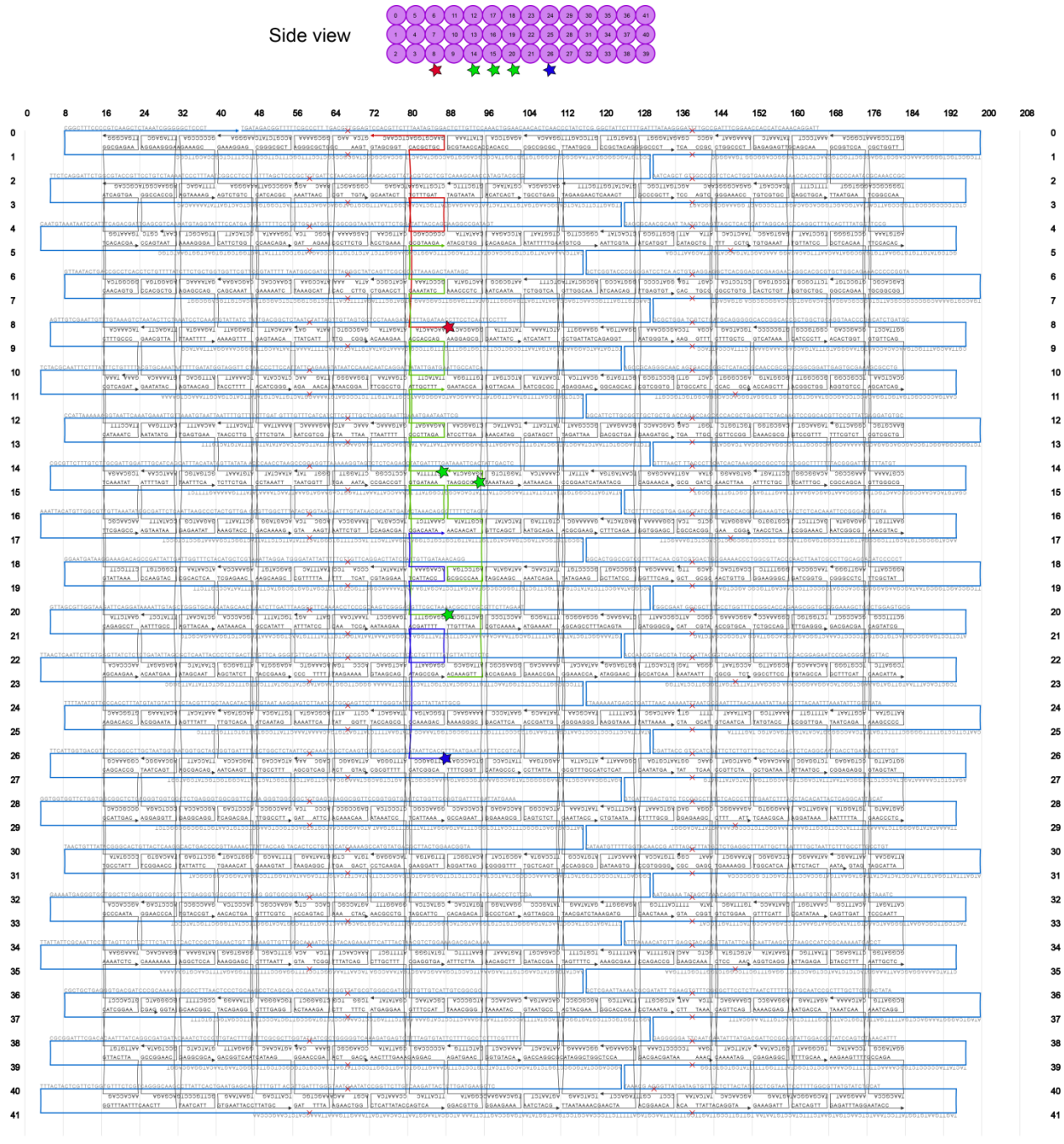

Figure S12: *Design file and DNA sequences of the origami structure from CaDNAno.*[10] *Helixes numbering of the side view drawing correspond to the left and right numbering of the design file. The staples modified with fluorophores are colored according to the spectral characteristics of the dyes (depicted as stars).*

SI 15 - Modified DNA strand

Strands R, G_1, G_3 and B are terminally modified with the desired fluorophore at the 5' end. An additional thymine base, shown as (T) in the table, was added to avoid quenching of fluorophores induced by the proximity with guanine and cytosine bases. Furthermore, fluorophores are known to stack via π-interaction of the aromatic rings with the DNA bases especially when DNA is in its double-stranded conformation[4] so the extra base acts also as a local single-stranded DNA to prevent stacking. Strand G_2 is internally modified, meaning Cy3 is linked to a thymine base.

Modified DNA strand	Name
cy5- (T)- AACAACTATCTTTGATCCGCCAGCCACGCTGCGAACGTGGACTCCAAC	R
cy3 -(T)-CCTTTTTAACCACCAGTTATACTTCAAATATCGCCCTAAAGCGTAAGA	G_3
ACAAAGTTAGTCCTGAGCGCCCAAGCGTTATATAAGGCGT-cy3-AGAGACTA	G_2
cy3 -(T)-GGAGGTTTGTGATAAACAAATTCTCCCTTAGAAAGAAGATATTGCTTT	G_1
Alexa488- (T)-CTTGAGCCACGATTTTGGAGAATTTCATTACCACAAGAAACGACAATA	B

Table S11: *modified DNA strands incorporated in the origami structure to construct the photonic wire.*

SI 16 – Cy5 properties in different FRET constructs

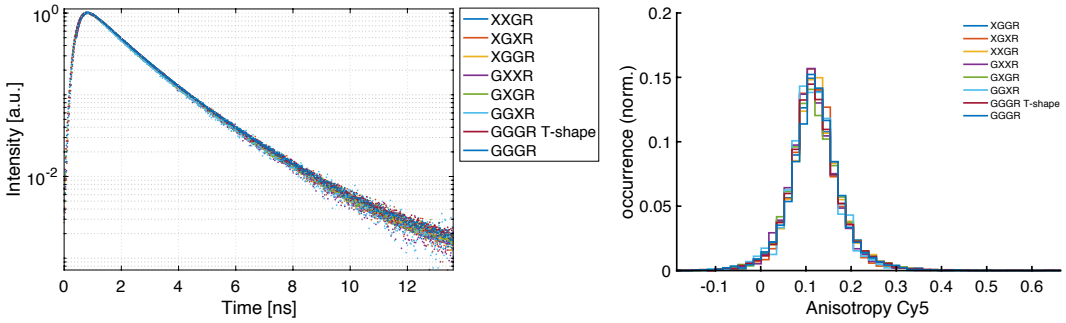

Figure SI 13: *Fluorescence decays of Cy5 after direct excitation and molecule-wise anisotropy histograms for all measured samples show that the acceptor behaves identically in all constructs.*

References

(1) Lakowicz, J. R. *Principles of Fluorescence Spectroscopy*; Lakowicz, J. R., Ed.; Springer US: Boston, MA, 2006.

(2) Sindbert, S.; Kalinin, S.; Nguyen, H.; Kienzler, A.; Clima, L.; Bannwarth, W.; Appel, B.; Müller, S.; Seidel, C. A. M. Accurate Distance Determination of Nucleic Acids via Förster Resonance Energy Transfer: Implications of Dye Linker Length and Rigidity. *J. Am. Chem. Soc.* **2011**, *133*, 2463–2480.

(3) Spiriti, J.; Binder, J. K.; Levitus, M.; van der Vaart, A. Cy3-DNA Stacking Interactions Strongly Depend on the Identity of the Terminal Basepair. *Biophys. J.* **2011**, *100*, 1049–1057.

(4) Sanborn, M. E.; Connolly, B. K.; Gurunathan, K.; Levitus, M. Fluorescence Properties and Photophysics of the Sulfoindocyanine Cy3 Linked Covalently to DNA. *J. Phys. Chem. B* **2007**, *111*, 11064–11074.

(5) Fischer, S.; Hartl, C.; Frank, K.; Rädler, J. O.; Liedl, T.; Nickel, B. Shape and Interhelical Spacing of DNA Origami Nanostructures Studied by Small-Angle X-Ray Scattering. *Nano Lett.* **2016**, *16*, 4282–4287.

(6) Bartell, L. S. On the Length of the Carbon-Carbon Single Bond. *J. Am. Chem. Soc.* **1959**, *81*, 3497–3498.

(7) Tomov, T. E.; Tsukanov, R.; Masoud, R.; Liber, M.; Plavner, N.; Nir, E. Disentangling Subpopulations in Single-Molecule FRET and ALEX Experiments with Photon Distribution Analysis. *Biophys. J.* **2012**, *102*, 1163–1173.

(8) Kudryavtsev, V.; Sikor, M.; Kalinin, S.; Mokranjac, D.; Seidel, C. A. M.; Lamb, D. C. Combining MFD and PIE for Accurate Single-Pair Förster Resonance Energy Transfer Measurements. *ChemPhysChem* **2012**, *13*, 1060–1078.

(9) Stennett, E. M. S.; Ciuba, M. A.; Lin, S.; Levitus, M. Demystifying PIFE: The Photophysics behind the Protein-Induced Fluorescence Enhancement Phenomenon in Cy3. *J. Phys. Chem. Lett.* **2015**, *6*, 1819–1823.

(10) Douglas, S. M.; Marblestone, A. H.; Teerapittayanon, S.; Vazquez, A.; Church, G. M.; Shih, W. M. Rapid Prototyping of 3D DNA-Origami Shapes with caDNAno. *Nucleic Acids Res.* **2009**, *37*, 5001–5006.